LA-UR -80-3142

TITLE: EVALUATION OF A CRYOSTABLE LOW-LOSS CONDUCTOR FOR PULSED FIELD APPLICATIONS

MASTER

AUTHOR(S): J. J. Wollan, Los Alamos Scientific Laboratory; M. S. Walker, B. A. Zietlin, and D. A. Pollack, Intermagnetics General Corporation; and S. S. Shen, Oak Ridge National Laboratory

SUBMITTED TO: Applied Superconductivity Conference, Santa Fe, NM, September 29-October 2, 1980

University of California

LOS ALAMOS SCIENTIFIC LABORATORY
Post Office Box 1663 Los Alamos, New Mexico 87545
An Affirmative Action/Equal Opportunity Employer

Form No. 836 R3
St. No. 2629
12/78

UNITED STATES
DEPARTMENT OF ENERGY

EVALUATION OF A CRYOSTABLE LOW-LOSS CONDUCTOR FOR PULSED FIELD APPLICATIONS*

John J. Wollan
Los Alamos Scientific Laboratory
Los Alamos, NM 87545

Michael S. Walker, Bruce A. Zeitlin, and D. A. Pollack
Intermagnetics General Corporation
Guilderland, NY 12084

S.S.Shen
Oak Ridge National Laboratory
Oak Ridge, TN 37830

Summary

A cryostable, low loss conductor as the basic strand in a 50 kA cable for a 20 MJ prototype, tokamak induction heating coil has been developed, fabricated, and evaluated. The conductor has a copper matrix multifilamentary NbTi core surrounded by a CuNi ring and stabilizing copper segmented by radial CuNi fins. Pulsed loss measurements have been made up to 2.2 T and for decay times from 1.7 to 278 ms. Measurements made on samples with various twists and portions etched away have allowed accurate evaluation of the loss components. Stability measurements were also made on insulated and uninsulated single strands and on subcables. Measured recovery heat flux for the bare strand is about 1.3 W cm^{-2}; however, the application of a 0.005 in. layer of Omega** insulation increases the value to about 1.5 W cm^{-2}.

Introduction

Induction heating coils of future tokamak devices will be required to produce 7 to 8 T fields which can be fully reversed in a few seconds. Energy requirements demand that the coils be superconducting. Engineering requirements demand that the coils be cryostable and exhibit low losses during cycling. Voltage and mechanical considerations require that the conductor current be at least 50 kA. This paper discusses the design, fabrication, and testing of two prototype strands for 50 kA cables which have been developed by Intermagnetics General Corporation (IGC) for the Tokamak Poloidal Field System program. The first phase of this program is the construction and testing of a 20 MJ prototype induction coil by Westinghouse for the Los Alamos Scientific Laboratory (LASL). The conductor for the 20 MJ coil is now being fabricated by IGC.

Conductor Design and Fabrication

The basic strand, shown in Fig. 1, is a low-loss, conductor which incorporates substantial copper for cryostability and a monolithic design that allows a thin, rugged, film insulation. A detailed description of the two prototype strands and the strand for the 20 MJ coil, all of which are configured essentially as shown in Fig. 1, is given in Table I. Prototype I was manufactured for Oak Ridge National Laboratory (ORNL) and Prototype II for LASL. The key differences in the strands are filament size, amount of niobium-titanium and copper-nickel, and the distribution of copper. The ORNL material was made from a 200 kg billet which

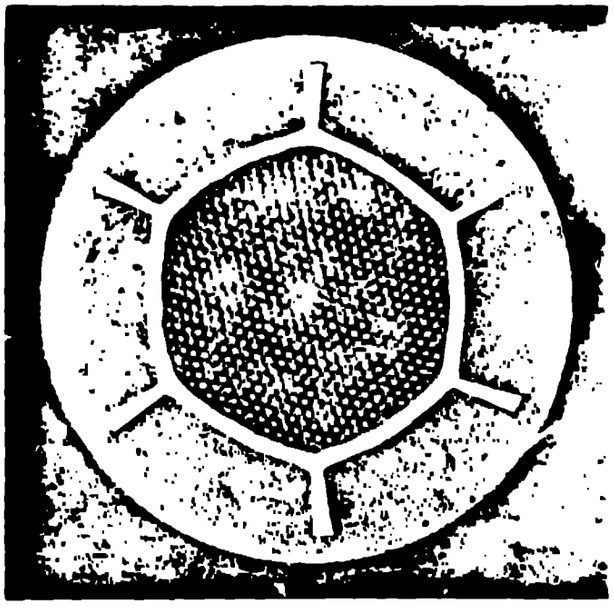

Fig. 1. Prototype II Strand

resulted in a filament size of 28.2 μm, whereas the LASL conductor was made from a 100 kg billet which resulted in 34.8 μm size. Starting materials for all conductors are OFHC copper with resistance ratio greater than 180 and annic high purity 90-10 copper-nickel. All elements were composed of fine grained materials, except for the copper-nickel shell in the ORNL conductor. Processing was basically standard, with two exceptions. First, because the filaments are clustered at the center of the conductor, the probability of fracture from center bursting is increased. Special dies were therefore used. It was felt the fins, however, would reduce the probability of center bursting, because they tend to make the strength of the composite more homogeneous. Second, to reduce the losses the twist pitch for Prototype II was reduced to 0.8/cm, only four times the overall diameter of the conductor. If the twist is referenced to the filament-filled region the pitch is 6.6 times this core diameter. The ability to twist tightly on a conductor of this form is a significant advantage of the design. We speculate that the very thick shell imposes hydrostatic body forces on the filaments during twisting which allows significant twist deformation without breaking the filaments.

Energy Losses

Energy loss measurements were made on Prototype I and II conductors having various twist and etched

*Work performed under the auspices of the U. S. Dept. of Energy.

**Westinghouse trademark.

TABLE I
CONDUCTOR STRAND DESCRIPTION

Item	Prototype I	Prototype II	20 MJ Coil
Metallic Radius, r_s	1.020 mm (0.0402")	1.029 mm (0.040[illegible]")	1.[illegible] mm (0.0[illegible]")
With Insulation, r_i	--	1.046 mm (0.0412")	1.046 mm (0.0[illegible]12")
Core Radius, r_c	0.695 mm (0.0273")	0.664 mm (0.0261")	0.660 mm (0.026[illegible]")
Filament Region r_f	0.641 mm (0.0252")	0.600 mm (0.0236")	0.600 mm (0.023[illegible]")
Fin Thickness, t_F	0.054 mm (0.0021")	0.066 mm (0.0026")	0.064 mm (0.00[illegible]")
Copper Shell, Δr	0.107 mm (0.0069")	0.098 mm (0.003[illegible]")	0.104 mm (0.00[illegible]")
Strand Twist, L_s	--	12.0 mm (0.472")	7.72 mm (0.304")
Cu Outer Area	1.681 mm^2 (51%)	1.782 mm^2 (54%)	1.825 mm^2 (56[illegible])
Cu Core Area	0.703 mm^2 (22%)	0.617 mm^2 (19%)	0.633 mm^2 (19[illegible])
Cu Total Area	2.384 mm^2 (73%)	2.399 mm^2 (73%)	2.458 mm^2 (75[illegible])
90 Cu-10 Ni Area	0.297 mm^2 (9%)	0.356 mm^2 (11%)	0.335 mm^2 (10%)
Nb Ti Area	0.588 mm^2 (18%)	0.514 mm^2 (16%)	0.476 mm^2 (15%)
Metal within r_s	3.269 mm^2 (100%)	3.269 mm^2 (100%)	3.269 mm^2 (100%)
Filament Size, d	28.2 μm	34.8 μm	22.1 μm
No. of Filaments, N_f	942	540	1,356

configurations. The objective of the measurements was to determine the distribution of the losses as a function of the various components of the conductor and to verify the reduction in losses with reduced twist pitch length. To reduce the losses in the 20 MJ coil to an acceptable level the twist pitch length was reduced to only four times the wire diameter. This pitch length produced no apparent degradation of the critical current or the electrical conduction in the stabilizer.

Hysteretic and dynamic losses were measured for an exponential field decay from starting fields of 2.2 to 0 T and for exponential decay time constants from 0.74 to 280 ms. Dynamic losses are defined as the difference between the measured losses for a slow field sweep from 0 to 2.2 to 0 T and a slow field sweep from 0 to 2.2 T followed by the rapid exponential change to 0 T.

The loss measurements on the prototype strands were analyzed to provide two pieces of information for design of the strands for the 20 MJ coil. The filament hysteresis losses shown in Fig. 2 provide values of critical current densities effective for losses at low field levels, and the dynamic losses shown in Figs. 3 and 4 confirm the transverse field coupling and eddy

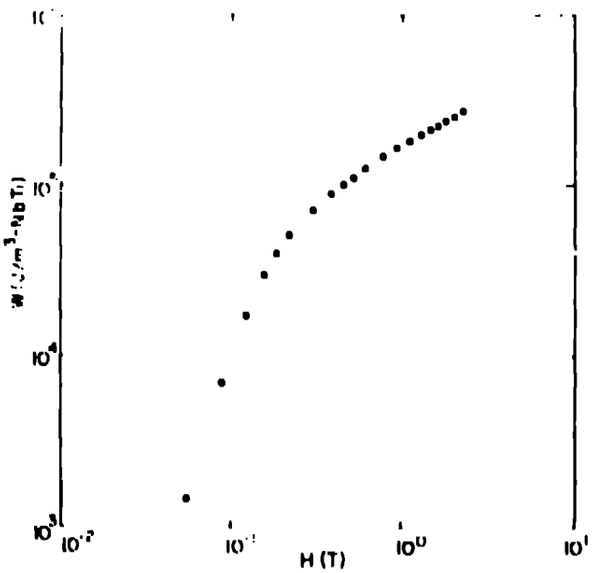

Fig. 2. Full cycle hysteresis loss, Prototype I strand.

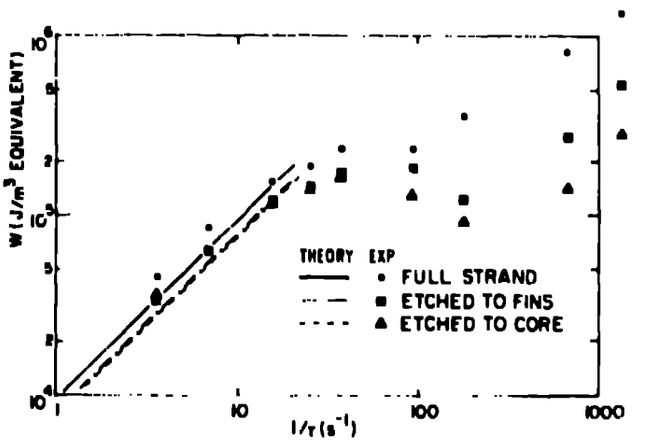

Fig. 3. Dynamic losses in Prototype I strand based on equivalent volume.

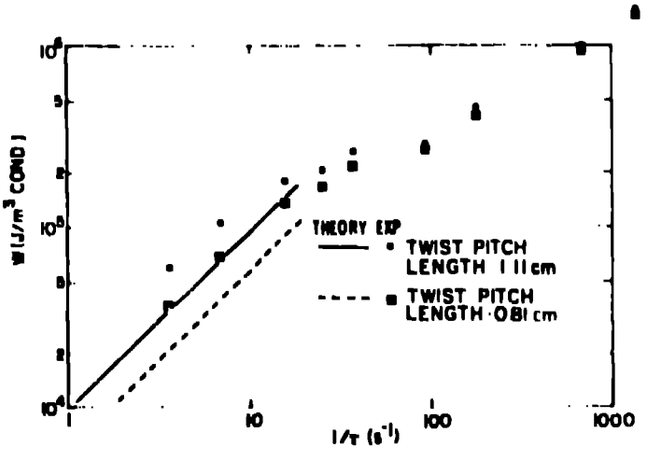

Fig. 4. Dynamic losses in Prototype II strand.

current loss theories. The correlation between the low field j_c values from transport current measurements, shown in Fig. 5, and j_c derived values from the loss measurement is poor. The measured cyclic loss per unit volume was accordingly used directly to project of losses near zero field for the 20 MJ coil.

The dynamic losses consist of coupling and eddy current components. For pulse times $\tau_\perp \ll \mu_o/2\rho_\perp (L/2\pi)^2$, these loss components are given by the low frequency instantaneous power loss expressions.[1,2]

$$\frac{P_c}{V_{strand}} = \left[\frac{\dot{B}_\perp L_s r_f}{2\pi r_s}\right]^2 \left[\frac{1}{\rho_\perp} + \frac{m}{\rho_r} + \frac{n}{\rho_{Cu,\ outer}}\right], \qquad (1)$$

and

$$\frac{P_e}{V_{strand}} = \frac{\dot{B}_\perp^2}{4\rho_{Cu,\ outer}} \left[\frac{r_s^4-(r_s-\Delta r)^4}{r_s^2} + 6\left(\frac{r_e}{r_s}\right)^4\right], \qquad (2)$$

respectively, where $\rho_\perp = (1+\lambda)/(1-\lambda)$ is the transverse resistivity in the core with λ the fraction of NbTi in the copper and NbTi core region and ρ_r is the resistivity of the copper-nickel ring and fins. The latter expression is the sum of conventional normal state eddy current losses for a cylindrical shell of thickness Δr and conventional normal state eddy current losses[3] in the six copper sectors within this ring and between the CuNi fins, each approximated as cylinders of equivalent single-sector area of radius r_e.

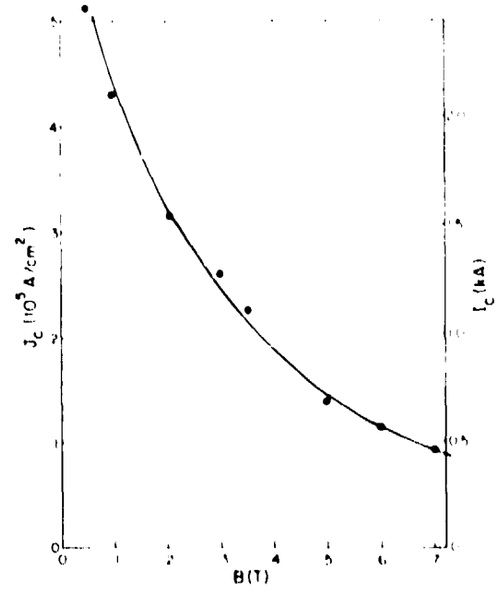

Fig. 5. Filament critical current density, Prototype I strand.

For the exponential field pulse from B_{max} to 0 with time constant τ, the integrated dynamic loss is

$$W_c = \frac{C_c(\rho_{Cu,\ core})}{\tau} \left[\frac{B_{max} L_s r_f}{2\pi r_s}\right]^2 \frac{1-\lambda}{1+\lambda}, \qquad (3)$$

and

$$W_e = \frac{C_e(\rho_{Cu,\ outer})}{\tau} \frac{B_{max}^2}{4} \left[\frac{r_s^4-(r_s-\Delta r)^4}{r_s^4} + 6\frac{r_e^4}{r_s^4}\right], \qquad (4)$$

where the second and third terms of equation (1) have been determined to be small due to the effectiveness of the CuNi ring and have been dropped from equation (3), and the coefficients,

$$C_c = \frac{1}{B_{max}^2\, \rho_{Cu,\ core}^{(B=0)}} \int_0^{B_{max}} \frac{B\,dB}{\left[1 + \frac{\Delta\rho(B)}{\rho_o}\right]_{core}}, \qquad (5)$$

and

$$C_e = \frac{1}{B_{max}^2\, \rho_{Cu,\ outer}^{(B=0)}} \int_0^{B_{max}} \frac{B\,dB}{\left[1 + \frac{\Delta\rho(B)}{\rho_o}\right]_{outer}}, \qquad (6)$$

were calculated for Prototype I using the copper resistivity ratios for the outer copper, $(\rho_{273\ K}/\rho_{20\ K})_{core} = 90$, and the copper between the filaments, $(\rho_{273\ K}/\rho_{20\ K})_{outer} = 125$, determined from resistivity ratio measurements in HNO_3 with the outer copper shell and the sectored region successively etched away. The total losses calculated for the Prototype I strands with these equations are about 20% below the measured losses for the full strand at $1/\tau$ values appropriately well below the $1/\tau$ upper limit of 100 s^{-1} for these strands. The calculated losses, excluding those in the outer copper shell and excluding the outer copper altogether, are similarly about 20% below the losses measured for the strands with the outer copper annulus etched away, and all of the outer copper etched away, respectively. This is good agreement with experiment, considering the judgments required for the use of conductor parameters and the approximations used in constructing the theory. The loss expressions used here and the method of their use are, therefore, confirmed. Note that the copper between the fins contributes a negligibly small loss component, and note also that the loss in the annulus is approximately half of what it would have been if the fins had not been present.

These same loss expressions were applied to the Prototype II strands using $RRR_{273} = 141$ for both the core and outer copper. As shown in Fig. 5 the predicted percentage loss reduction due to twist is achieved, but the absolute value of the losses projected for both pitch lengths is lower than that measured by about 40%. The effect of twist length has

thus been confirmed for tight twists of the type that will be used in the 20 MJ coil. Because the filament size and number will be more like that in Prototype I, and these parameters influence the effect of ρ_{Cu} and λ, the values used in calculating losses for Prototype I have been used for the 20 MJ coil design.

Conductor Stability

Stability measurements have been made on the Prototype I strand, bare and insulated, and insulated Prototype II strands in a six-around-one subcable. Heaters mounted on the samples induced a normal zone in the conductor and voltage taps were used to monitor its subsequent propagation or recovery. Details of the experimental approach have been discussed.[4]

The samples were wound on a 20 cm diameter G-10 cylinder in a way which essentially allowed total surface contact to LHe. Heaters were 0.64 cm by 5.1 cm by 0.025 cm Kapton covered resistance strips. For the single strand samples the heater was wrapped on a 0.5 cm diam, 0.9 cm long copper cylinder, soldered to the conductor. For the subcable the heater was simply wrapped around and taped. Heater powers, a few watts, were the minimum required to drive the sample normal.

Results of stability current measurements on the Prototype I strand are given in Table II. Stability or recovery current is defined here as the maximum current that the conductor can carry and still recover to the superconducting state after the removal of a minimum, steady state heat input which produces a normal zone. A significant enhancement in heat transfer and consequently recovery current for the insulated compared to the bare strand is seen. The respective heat transfer rates, calculated simply as $I^2\rho(B)/A_{Cu}P$ where P is the total strand perimeter, are approximately 0.5 W/cm^2 and 0.3 W/cm^2.

Results on the Prototype II subcable are also given in Table II. The heat transfer rate cannot be obtained directly from the data because the surface area available for cooling is unknown. If, however, the heat transfer is assumed to be unchanged, then the fraction of surface area per strand which is available for cooling can be calculated. This is roughly 60% as shown in the bottom row of Table II. Extrapolation, which ignores further loss of surface heat transfer area due to final cabling and spacers, of the subcable recovery current data to the full 50 kA cable for the 20 MJ coil gives 66 kA. Configuration effects are to be evaluated in a test of the full 50 kA prototype cable in the Lawrence Livermore Laboratory High Field Test Facility.

TABLE II
SINGLE STRAND RECOVERY CURRENT

	Field (T)								
	0	2.0	3.0	3.8	4.2	4.5	5.0	5.5	5.7
Bare	630	490	430	400	380	380	370	360	350
Insulated	820	670	590	560	515	510	470	460	450

SUBCABLE RECOVERY CURRENT (Insulated Strands)

	Field (T)					
	3.0	4.0	5.0	5.5	5.7	6.0
Recovery	2650	2450	2250	2200	2150	2100
$\frac{(i_{subcable}/6)^2}{I^2_{strand}}$	0.56	0.56	0.64	0.64	0.63	—

Two other aspects of the recovery characteristics of the conductor were investigated. First, the recovery current as a function of LHe bath temperature was measured at 4 T. The dewar was allowed to pressurize and the bath temperature to rise from the ambient 4.0 K to about 4.5 K, the operating temperature of the 20 MJ coil. There was no measurable change in the recovery current. Second, the conductor recovery characteristics under pulsed heat input conditions above the steady state recovery limit were also measured at 4 T. Initially the energy required to produce a normal zone as a function of pulse time was determined. This energy became constant below 50 ms, which was then chosen as the pulse width. The results shown in Fig. 6 define the cryostable limit from above and agree well with the steady state limit.

Conclusions

Cryostable, low-loss strands for cables for pulsed coil applications have been successfully fabricated. Energy loss and stability measurements and analysis show that the strands meet the requirements for a 20 MJ prototype tokamak induction heating coil. The thin, tough insulation desirable for induction coil cyclic operation, made possible through the use of uniquely configured monolithic strands, achieves a substantially increased heat transfer over that provided by bare wire surfaces.

References

1. J. H. Murphy and M. S. Walker, Advances in Cryogenic Engineering, 24, p. 406 (1978).
2. B. Turck, J. Appl. Phys. 50, p. 5397 (1979).
3. W. A. Fietz, IEEE Trans. MAG 13, p. 807 (1977).
4. R. I. Schermer, IEEE Trans. MAG 15, p. 355 (1979).

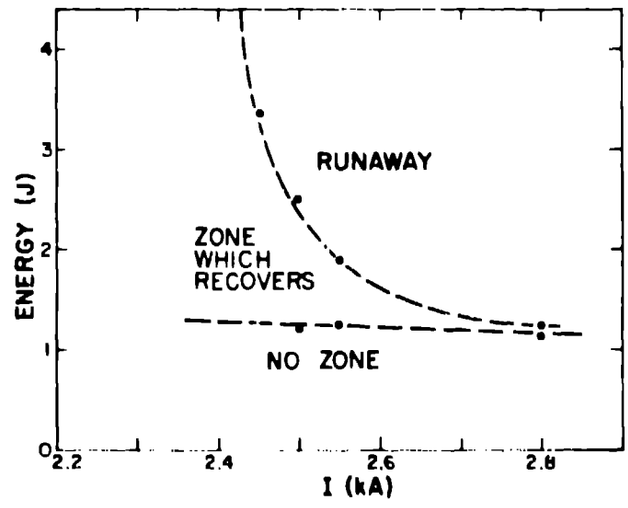

Fig. 6. Recovery characteristics above cryostable limit.